Exploration of Gas Reservoir Modeling Technology and Its Application in Sulige Gas Field: A Case of Sudong-X Reservoir

You Zhou[1,2](✉), Yu-qi Bai[1,2], Bin Fu[1,2], Yu-fei Wang[1,2], Yi Wang[1,2], and Zhan-hai Yu[1,2]

[1] Exploration and Development Research, Changqing Oilfield, Xi'an, Shanxi, China
zhouyou_cq@petrochina.com.cn
[2] State Engineering Laboratory of Exploration and Development for Low-Permeability Oil and Gas Fields, Xi'an, Shanxi, China

Abstract. Underground Gas Storage (UGS) is the main facility to ensure the safe supply of natural gas and an important part of national energy security. Changqing Oilfield actively responds to the call and selects well area X in the eastern part of Surige Gas Field as the target of gas storage construction. The gas reservoir in this well area is well developed in the lower Paleozoic Ordovician $Ma_5{}^5$, which is a depleted oil and gas reservoir with pore permeable formation of original saturated oil and gas water as the storage medium. In order to learn the reservoir distribution pattern deeply and accurately describe the spatial distribution of reservoir properties and the non-homogeneous characteristics of the reservoir, a multi-data fusion 3D geological model is established using a differentiated modeling method. This precise geological model can be used as a guide to conduct research and application of optimal well location deployment of injection and extraction well, which provides a basis for the construction of gas storage.

Keywords: Underground Gas Storage · Lower Paleozoic · 3D Geological Model · Non-integrating surface

J. Lin (Ed.): IFEDC 2023, SSGG, pp. 879–889, 2024.
https://doi.org/10.1007/978-981-97-0268-8_69

1 Introduction

With the rapid growth of natural gas consumption as a clean, efficient and high-quality energy source in recent years, the demand for gas storage and peak regulation has been increasing day by day [1]. In order to ensure China's energy security, coordinate resources and market supply and demand relationships, and accelerate the development of the natural gas industry in the Changqing gas field, the construction of gas storage facilities is imperative.

The underground gas storage facilities in the world are mainly divided into several types, including depleted oil and gas reservoirs, aquifers, salt caverns, and abandoned mines. Among them, the depleted oil and gas reservoir type gas storage facilities account for the highest proportion in the gas storage facilities due to their large storage capacity and the availability of existing facilities in oil and gas fields [2, 3]. The Sudong X Well area belongs to the depleted gas reservoir-type gas storage facility. This type uses the porous permeable strata of original saturated oil, gas and water as the storage medium. Therefore, the distribution and heterogeneity of the reservoir determine the storage capacity and injection and production efficiency of the gas storage facility [4, 5]. A three-dimensional geological model is undoubtedly a good means of characterizing the anisotropy and multiple properties of the strata. The establishment of the model can guide the deployment of injection and production wells, simulate the injection and production process, and optimize the injection and production scheme to better play the role of the gas storage facility.

2 Basic Geological Characteristics of Gas Reservoirs

2.1 Well Area Overview

The Sulige gas field is located in the Sulige Temple area on the west side of the Jingbian gas field in the Ordos Basin. It is administratively under the Wushen Banner and Etoke Banner of the Inner Mongolia Autonomous Region. The exploration area starts from Qianqi of Etoke Banner in Inner Mongolia to Taolimiao in Shaanxi, and to Aobagajin in Etoke Banner of the back of Etoke Banner in the north. The total exploration area is about 55 000 km^2. It is a typical ultra-large tight gas field with low pressure, low permeability, and low abundance discovered on land in China [6]. The Sudong-X well area is located in the middle of the eastern area of the Sulige gas field. The structural zoning belongs to the Yishan Slope Structural Unit of the Ordos Basin. The surface is desert and grassland, and the terrain is relatively flat, with an altitude of about 1 300 m (Fig. 1).

The development target layer of the Lower Paleozoic in the research area is the Ma_5 of the Majiagou Formation of the Ordovician, which is composed of carbonate rocks. The reservoir is composed of fine crystal to medium crystal dolomite, and the surrounding area is developed with tight mud crystal limestone [7, 8]. The gas reservoir is buried at a depth of 3 100 to 3 160 m, with a small scale and a lens-shaped structure, belonging to a typical lithologic trap gas reservoir.

A total of 12 gas wells were drilled in the Lower Paleozoic Majiagou Formation in the study area (excluding injection and production test wells). Among them, 12 wells were

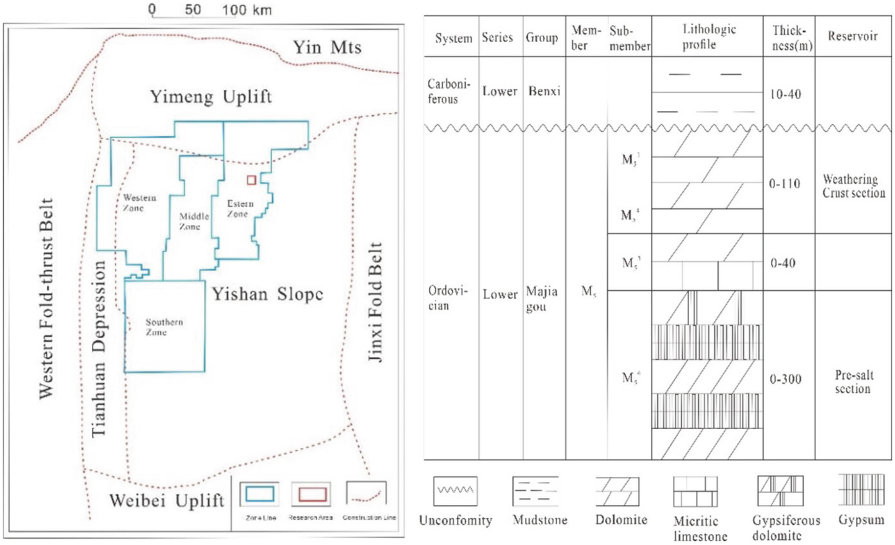

Fig. 1. (Left) Location of Research Area; (Right) Composite stratigraphic column of M_5 Member in mid-east of the basin.

drilled to the Ma_5^5 (including two horizontal wells), and 12 wells encountered effective reservoirs of the Ma_5, with a thickness of 4.0 to 28.7 m and an average thickness of 14.0 m. The effective reservoir thickness ranges from 0.8 to 21.8 m, with an average effective thickness of 9.2 m. The average porosity is 8.66%, the average matrix permeability is

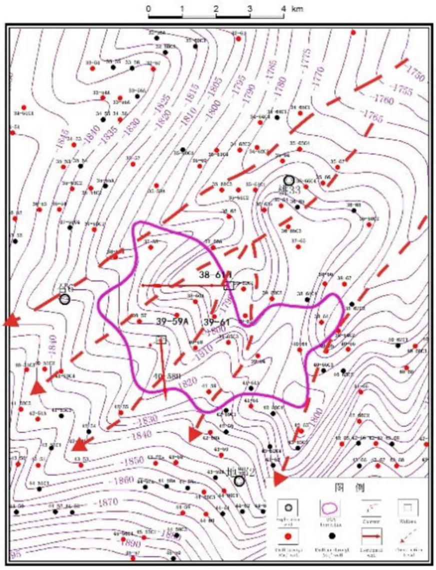

Fig. 2. Structural Map of top Ma_5^5 in Sudong X well area

13.68×10^{-3} μm^2, and the average gas saturation is 71.33%. The predicted area of the gas reservoir is 21.2 km^2, and the geological reserves are about 2.78 billion cubic meters (Fig. 2).

2.2 Reservoir Structure Characteristics

The Sulige gas field is located in the northeast of the Yishan slope of the Ordos Basin. After experiencing the Indosinian and Yanshan movements, it was overall reversed to the west-dipping monocline that uplifts to the east. It extends north-south and is characterized by a regional west-dipping monocline with a slope of 7–10 m/km^2 and a dip angle of less than 1°. On the extremely gentle structural background, a series of small north-northeast to south-southwest oriented and alternately arranged small anticlines and synclines are distributed on the west-dipping monocline, which are commonly known as "nose highs" and "nose lows," with a main orientation of northeast.

The study area is located in the middle and southern part of the eastern region of the Sulige gas field and is situated in a large nose high area under the gentle west-dipping monocline of the Ma5 formation. Specifically, there are four axial NE-SW nose highs on the west-dipping monocline in the study area. At the same time, the area has been subjected to strong NW-SE tectonic compression, and the local tectonic amplitude is relatively large, with a dip angle of about 0.15–1°. The Ma_5 gas layer in this area is buried at a depth of 3 100 m–3 160 m, with a top elevation of −1 780 m–1 850 m.

2.3 Reservoir Spreading Characteristics

Plain Display Characteristics

Based on core observation and logging interpretation results, the thickness of the Ma5 dolomite in the study area was statistically analyzed. The dolomite is distributed in a lenticular shape and is mainly controlled by sedimentary facies. It is mostly distributed in Yunping and clastic flats, appearing as bead-like or lenticular bodies on the plane, mainly concentrated near Sudong-X well section. At the same time, the distribution range of dolomite expands from the Ma_5^5 sub-Sect. 3 to Ma_5^5 sub-Sect. 1.

Vertical Display Characteristics

The Ma_5^2 dolomite gas reservoir in the study area is a lithologic trap gas reservoir, controlled by sedimentary facies, and is distributed in a lenticular shape with poor continuity, small in size, and vertically reflecting a relatively developed Ma_5^2 effective reservoir (Fig. 3).

Reservoir Non-homogeneity

The internal connectivity of the reservoir in this area is good, but the heterogeneity of the reservoir is strong. The cross-section shows that the lithology and thickness of the dolomite reservoir in the short-range also have significant differences. The heterogeneity index of the reservoir in this area also reflects that the reservoir has strong heterogeneity: the coefficient of variation of permeability is 1.06, which is of the non-uniform type; the permeability range is 911.76, and the heterogeneity coefficient is 1 to 911.76 (Table 1).

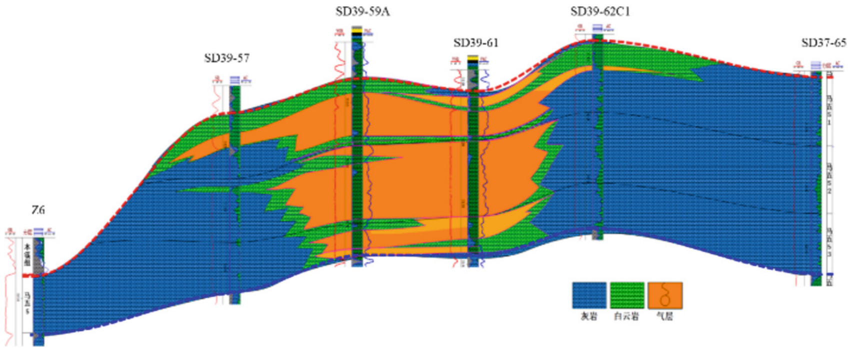

Fig. 3. $Ma_5{}^5$ reservoir isogram gas reservoir cross-section

On the plane, it is mainly manifested as a large difference in reservoir permeability between the center and the edge, which is also reflected in the production capacity of individual wells.

Table 1. Non-homogeneity index of $Ma_5{}^5$ reservoir

Mutant indicator	Scope	Average	Notes
Permeability coefficient variation		1.06	≤0.5 is uniform; 0.5–0.7 is more uniform; ≥0.7 is uneven
Permeability Range		911.76	The closer to 1, the more homogeneous the reservoir is
Non-homogeneity coefficient	1–911.76	143.66	

3 Three-Dimensional Geological Modeling

Based on the research of the gas storage area, the Petrel software was used to establish a structural, lithological, and attribute model for the Ma_5 formation of the Ordovician system and its cap and bottom plates, and reserves were calculated. The model comprehensively and intuitively reflects the distribution and physical properties of the reservoir in the storage area, and also provides a solid basis for numerical simulation and injection-production well deployment.

3.1 Grid System

The plane grid unit is 30 × 30 m, which has a good display of the boundary shape of the dolomite body. It is divided into 30 layers vertically, with an average layer thickness of less than 1 m. The total number of Ma_5 layer grid nodes in the study area reaches 2.6 million, and the total number of geological model grid nodes including cap and bottom plates reaches 15 million.

3.2 Tectonic Model

The Ma_5 formation in the objective layer is fully exposed in the study area, and it is complete in the structural model. However, there are different degrees of loss of the Ma_4 and Ma_3 formations above the Ma_5 and they are unconformably in contact with the overlying Benxi formation. In order to better depict the stratigraphic erosion surface, the method of combining seismic interpretation of structural surfaces in the study area with the artificial depiction of structural surfaces to constrain well-point layering data was used to obtain the structural surfaces of each small layer, and local tectonic anomaly points were adjusted by human-computer interaction. The erosion surface was effectively presented, and the unconformable contact relationship between the strata was restored based on the structure-established stratigraphic model depth (Fig. 4).

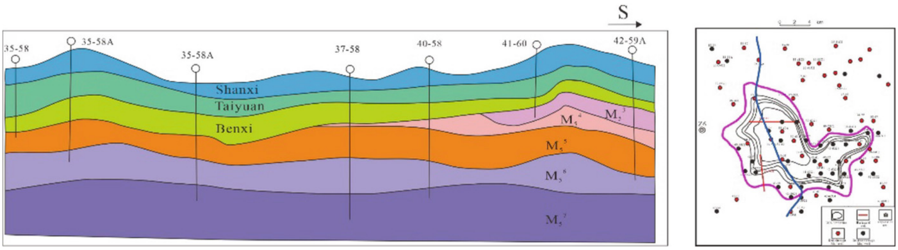

Fig. 4. Comparative N-S stratigraphic section

3.3 Petrographic Model

Different sedimentary backgrounds have different morphological distributions of lithofacies. Therefore, a differential modeling method was used to better display the distribution of lithofacies.

In the upper Paleozoic strata (Shanxi Formation, Taiyuan Formation, and Benxi Formation), the sedimentary environment is mainly characterized by fluvial and tidal flat deposits, with good continuity of sand bodies distributed along the river channels [12]. The variogram model adopted a spherical model, and the sequential indicator simulation method was used to establish lithofacies models, which can better display the continuity of sand bodies.

In the lower Paleozoic strata (Majiagou Formation), the sedimentary environment is mainly composed of evaporative tidal flat deposits, with the same lithofacies slices and clear boundaries [13]. To improve the consistency between the model and geological knowledge, the Gaussian model was used for the variogram analysis, and the truncated Gaussian simulation method was used to establish the lithofacies model under the constraint of the distribution of dolomite in the core area. This method is beneficial to describe the boundaries of reservoirs.

The model shows that the distribution of sandstone and mudstone in the upper strata can be used to depict the direction of river channels. The dolomite in the core area of the lower strata is the main reservoir, and the limestone has good sealing properties. The distribution area of the upper part is larger than that of the lower part, which is consistent with the geological knowledge and provides a detailed description of heterogeneity. The thickness ranges mainly from 0 to 30 m, which is consistent with the core thickness range of the wells in the area and mainly concentrated in the core well area near 39-59A, 39-61, and 39-64 wells (Figs. 5 and 6).

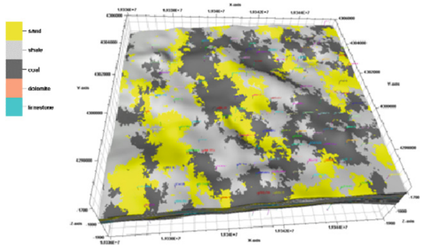

Fig. 5. Full view of the petrographic model of the $Shan_2{}^3$-Benxi Formation

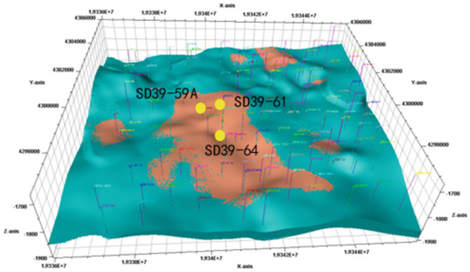

Fig. 6. Full view of the petrographic model of the Majiagou Formation

3.4 Attribute Model

From a statistical point of view, facies-controlled modeling divides a sample area into small blocks of varying sizes based on certain properties of the sample, and then uses random simulation methods to obtain the best simulation sample distribution by performing random interpolation in each small block. From a geological point of view, the premise of facies-controlled property modeling is that the reservoir parameters of different facies belts have different expected values and variances due to diagenesis, and therefore their spatial correlation is also different. Therefore, when interpolating the physical property parameters, simulations need to be performed separately based on the facies types they belong to [14].

After converting the porosity interpretation data from the logging curves into coarse data, the input data was subjected to truncation transformation, removal of outliers, and normalization. The data was then divided into small layers, lithofacies, and normal distributions of each property obtained. Then, the variogram function analysis was carried out for different lithofacies belts in each layer, and finally, the porosity model was established using the sequential Gaussian simulation method with lithofacies as a constraint. This method is fast and simple and is suitable for simulating physical properties with continuous intermediate values and dispersed extreme values [15, 16].

The distribution of permeability and saturation is similar to that of porosity, but the former values are generally not normally distributed and need to be subjected to truncation transformation and outlier removal [17]. Finally, using lithofacies as a constraint condition and the porosity model as the second data body, the permeability model was established using the collaborative sequential Gaussian simulation method.

The porosity range of the model is between 0.5% and 15%, and the porosity in the core area is significantly higher, averaging around 10%. The permeability range varies greatly, with the maximum predicted value between wells reaching over 10×10^{-3} μm^2. The overall saturation is high, concentrated between 60% and 80%. The distribution of both property values is in good agreement with porosity, and high values are concentrated near the well areas of SD3961, SD39-59A, and SD38-60A, indicating the main gas-bearing area.

4 Geological Model Validation and Application

4.1 Reserve Calculation

The geological model was used for reserve calculation, with the lower limit of porosity set at 2%, the lower limit of permeability at 0.01 mD, the lower limit of gas saturation at 50%, and the natural gas volume coefficient at 0.004. The relative error of the calculated reserves is −1.4%, and the fitting degree is relatively high.

4.2 Historical Matching

The non-equilibrium initialization method was chosen to determine the distribution of reservoir oil, gas, water, and pressure. The numerical simulation boundary was set at the boundary of the dolomite, without coarsening the geological model. The bottomhole pressure and daily gas production of the six gas wells in the core area were directly fitted, with a fitting degree of up to 83%, only SD39-62C3 had a poor fitting effect. The reason for this is that the well is located at the edge of the core area, the gas well has a long production history, and the matching between gas well pressure and gas production is poor (Fig. 7).

4.3 Model Application

Scheme Optimization
Considering the later management and implementation risks, the full vertical/directional wells and full horizontal wells are not applicable. This article focuses on using the model to compare and screen the hybrid well pattern scheme.

Hybrid well pattern scheme 1:11 vertical/directional wells and 3 horizontal wells. Deploy and implement vertical/directional wells in the core area to facilitate the rapid

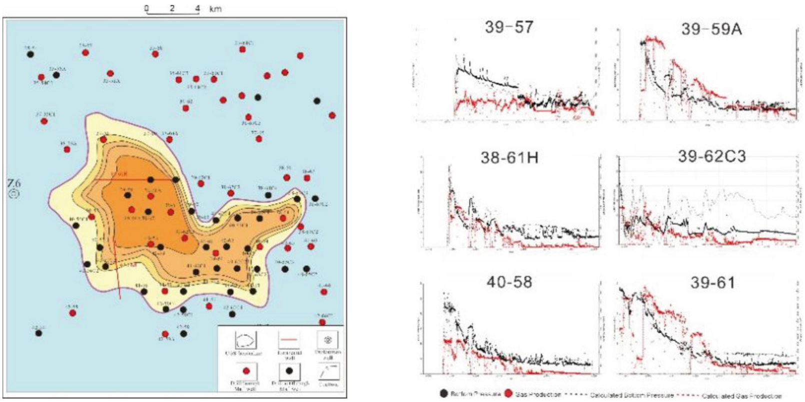

Fig. 7. Core area historical fitted well locations and fitting maps

recovery of formation pressure after gas injection. The properties gradually worsen from the inside out, and horizontal wells are deployed in areas with relatively poor properties, which can improve gas well production and have relatively low risks.

Hybrid well pattern scheme 2:12 vertical/directional wells and 4 horizontal wells. There is one less vertical/directional well in the core area than in scheme 3, and the recovery of formation pressure after gas injection is relatively slow. The horizontal wells are located in the core area, with less risk and less extended horizontal sections, which limits production capacity.

Based on the three-dimensional geological model, the production situation during the gas production stage of the gas storage was simulated, and both gas storage schemes can meet the working gas requirements. However, in scheme 1, the pressure drop in the core area is more uniform at the end of the gas storage period, and the reserves are fully utilized (Fig. 8).

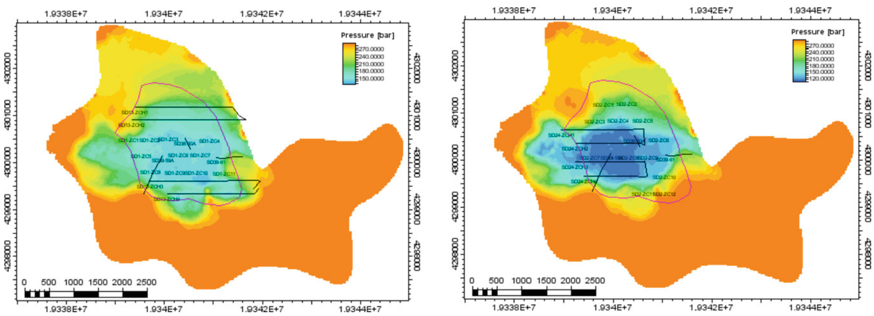

Fig. 8. Well deployment scenarios and formation pressure distribution at the end of gas recovery from the gas reservoir (left: scheme 1, right: scheme 2)

Horizontal Well Deployment

The established lithofacies and gas saturation models were used to guide the deployment of injection and production wells, designing targets in reservoirs with good properties and controlling the trajectory of horizontal wells to move through the effective reservoirs (Fig. 9).

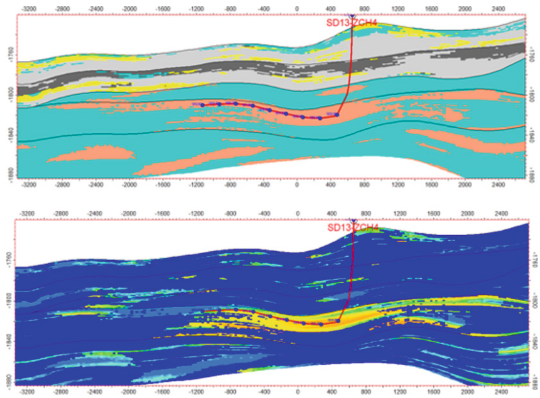

Fig. 9. Horizontal well trajectory petrographic (top) and gas saturation (bottom) profiles

5 Conclusions

1. For the first time in China, a three-dimensional geological model was used to design injection and production schemes and deploy injection and production wells in gas storage, and the accuracy of the model was verified to be above 80% using reserve calculation and historical gas well production fitting methods.
2. To restore the unconformable contact relationship between strata in an eroded stratum, a combination of seismic interpretation of structural surfaces and artificial drawing of structural surfaces was used to constrain the well point layer data, which can restore the unconformable contact relationship between strata more realistically.
3. Different sedimentary backgrounds correspond to different lithofacies distribution patterns, and differential modeling methods were used to better display the lithofacies distribution patterns.
   (1) Ancient layers (Shan23, Taiyuan, Benxi Formation) are mainly composed of fluvial and tidal flat deposits, with good sand body continuity and distributed along the river channel direction. The variogram model used is the spherical model, while the sequential indicator simulation method is used for lithofacies modeling.
   (2) The lower ancient layers are mainly composed of evaporite tidal flat deposits, with the same lithofacies developed in contiguous slices and clear boundaries. The Gaussian model was used in the variogram function analysis. Under the constraint of the distribution of dolomite in the core area, the truncated Gaussian simulation method was used to establish the lithofacies model.

References

1. Ding, G.S., Wei, H.: Review and outlook of 20 years of underground gas storage construction in China. Oil Gas Storage Transp. **39**(373(01)), 25–31 (2020)
2. Ding, G.S., et al.: Current status and technology development direction of underground gas storage in China. Nat. Gas Ind. **35**(265(11)), 107–112 (2015)
3. Ma, X.H., Zheng, D.W., Shen, R.C., et al.: Key technologies and practices of gas reservoir-based storage construction in complex geological conditions in China. Petrol. Exp. Dev. **45**(264(03)), 489–499 (2018)
4. Wen, K., He, L., Yu, W.C., et al.: Calculation methods on formation pressure of underground gas storage rebuilt from depleted oil and gas reservoir. Oil Gas Storage Transp. (2017)
5. He, Z.Q., He, T., Yi, W.K., et al.: Gas reservoir injection and extraction technology and development suggestions for depleted gas reservoirs in Sinopec. Geol. Exp. **56**(491(03)), 605–613 (2020)
6. Li, J.B., Fu, B., Zhao, Z.J., et al.: Reservoir characterization technology of dense sandstone gas reservoir in Surig gas field and its development prospect. Nat. Gas Ind. **35**(266(12)), 35–41 (2015)
7. Bai, H., Yang, T.B., Hou, K.F., et al.: Main control factors and enrichment zone preference of Ma Wu_5 gas reservoir in the eastern part of Sulige gas field. Xinjiang Petrol. Geol. **43**(216(03)), 271–277 (2022)
8. Wei, X.S., Chen, J.P., Zhang, D.F., et al.: Analysis of geological characteristics and reservoir formation conditions of large area of dense carbonate gas in the eastern Ordos Basin. Nat. Gas Geosci. **28**(5), 677–686 (2017)
9. Yang, H., Liu, X.S., Zhang, D.A.F.: Main control factors and exploration progress of natural gas formation in Ordos Basin Ordovician marine carbonates. Nat. Gas Ind. **33**(5), 1–12 (2013)
10. Zhang, C.L., Liu, X.S., Yang, Y.J., et al.: History and inspiration of oil and gas exploration in Changqing oil field in Ordos Basin. Xinjiang Petrol. Geol. **42**(3), 253–263 (2021)
11. Xie, J.L., Wu, X.N., Sun, L.Y., et al.: Prediction of petrographic paleogeography and favorable zones in five sections of the Ordosian Majiagou Formation in Ordos Basin. Offshore Oil Gas Geol. **18**(4), 23–32 (2013)
12. Ma, Z.X., Wu, Z., Zhang, J., et al.: Characterization of braided river reservoir configuration and geological modeling technology based on dynamic and static information fusion. Nat. Gas Ind. **42**(339(01)), 146–158 (2022)
13. Hu, X.Y., Li, Y., Quan, L.S., et al.: Three-dimensional geological modeling method for carbonate suture-hole type reservoirs–a case study of Ordovician reservoirs in Tahe Oilfield IV. Petrol. Nat. Gas Geol. **34**(03), 383–387 (2013)
14. Wu, S.H.: Reservoir Characterization and Modeling. Petroleum Industry Press. ISBN 978-7-5021-7590-0
15. Chen, C.H., Chang, R., Yang, F.: Research on fine description and 3D geological modeling of reservoir reservoir in Surig gas field. Petroch. Appl. **35**(176(07)), 92–95 (2016)
16. Yang, R.C., Wang, Y.L., Fan, A.P., et al.: Geological modeling of reservoir in Z30 block of Surig gas field in Ordos Basin. Nat. Gas Geosci. **23**(124(06)), 1148–1154 (2012)
17. Palermo, D., Aigner, T., Seyfang, B., et al.: Reservoir properties and petrophysical modelling of carbonate sand bodies: outcrop analogue study in an epicontinental basin (Triassic, Germany). Geol. Soc. Lond. Spec. Publ. **370**(1), 111–138 (2012)
18. Liu, L.L., Xu, W., Shi, S.H., et al.: Effective reservoir modeling approach for tight sandstone gas reservoirs in Surig gas field. Oil Gas Geol. Recovery **22**(114(03)), 47–51 (2015)
19. Zheng, D.W., Xu, H.C., Wang, J.M., et al.: Key technologies for reservoir-based gas storage construction and evaluation. Petrol. Exp. Dev. **44**(260(05)), 794–801 (2017)